Journal of Sustainable Mining 18 (2019) 142–149

HOSTED BY

ELSEVIER

Contents lists available at ScienceDirect

Journal of Sustainable Mining

journal homepage: www.elsevier.com/locate/jsm

Research paper

Long-term prediction of non-processed waste radioactivity of a niobium mine in Brazil

Thammiris Mohamad El Hajj[a], Mauro Pietro Angelo Gandolla[b], Paulo Sergio Cardoso da Silva[c,*], Henrique Torquato[d], Homero Delboni Junior[e]

[a] Universidade Federal de Alfenas (UNIFAL-MG), Rodovia José Aurélio Vilela, 11999, Poços de Caldas, Brazil
[b] ECONS S/A, Via Stazione 19, Bioggio, Switzerland
[c] Instituto de Pesquisas Energéticas e Nucleares (IPEN), Av. Prof. Lineu Prestes, 2242, São Paulo, Brazil
[d] CMOC International, Rodovia BR 050, Km 271, Catalão, Brazil
[e] Universidade de São Paulo (USP), Rua Professor Melo Moraes, 2373, São Paulo, Brazil

ARTICLE INFO

Keywords:
NORM
Radiological hazard indices
Waste re-use
Radiation protection
Niobium ore

ABSTRACT

This work analyzed samples from a niobium mine in Brazil which produces massive quantities of non-processed waste (NPW) each year. Due to concerns about the environmental impact of stacking up this material in the long-term, investigations have had been made to evaluate its re-use options. Nevertheless, there are no regulations from the Brazilian National Commission of Nuclear Energy about commercializing this sub-product which has highly variable radiological activity because of the different lithologies present in the mine. Thus, the activity concentrations of ^{238}U, ^{232}Th, ^{226}Ra, ^{228}Ra, ^{228}Th and ^{40}K of the naturally radioactive ore (53 boreholes) and of the NPW (8 samples) were measured. Radiological hazard indices, radium equivalent, internal and external hazard and their equivalent doses were also calculated. Moreover, the X-ray diffraction, depth and coordinates of all samples were used to identify radioactive prone areas in the mine. For the NPW samples, the activity concentrations (in Bq/kg) were, on average, 64.9 of ^{238}U, 104.8 of ^{226}Ra, 1813.9 of ^{232}Th, 1292.2 of ^{228}Th, 1224.3 of ^{228}Ra and 1184.2 of ^{40}K. The analysis showed great variability between samples and the results can be used to evaluate possible uses such as building materials or foundation for roadbeds.

1. Overview

Anthropogenic sources of radiation, including naturally occurring radionuclides that might be released into the environment as a result of human activity, are one of the main concerns when it comes to environmental radiological protection. Although naturally occurring radionuclides are of primordial origin, exposure to them cannot be neglected in an assessment of environmental impact (Vives i Batlle, Ulanovsky, & Copplestone, 2017; EC, FAO, ILO, OECD/NEA, PAHO, UNEP, WHO, 2014). Niobium ore has been listed worldwide as Naturally Occurring Radioactive Material (NORM) (Liu & Pan, 2011; Ferrira, da Silva, Lima, & da Silva, 2018; International Atomic Energy Agency, 2013) which makes the handling of the waste and tailings more challenging from an environmental perspective. The only two countries with relevant niobium ore reserves are Brazil and Canada. There are a few other occurrences in Australia, USA and Africa, but together they represent 1% of the total production. Brazil is the world leader in the production of ferroniobium, with a share of the market reaching up to 90% and the demand increases each year because this metal is widely used in superalloys, superconducting magnets and in medical and jewelry applications due to its hypoallergenic properties (Departamento Nacional de Produção Mineral., 2018; Garcia C Marques, Mohamad El Hajj, Maques Braga Junior, Chieregati, & Delboni Junior, 2017; Gonçalves de Lima, 2010; Rangel Alves, 2015).

According to Josef Maringer et al. (2017), industries working with NORM raw materials produce large amounts of waste and such waste materials constitute a huge economic and ecological burden if not properly disposed of or re-used. In addition, as resources consumption continues to increase, energy consumption (mainly in the milling process), diesel use and process recovery are major issues in the mining sector regarding sustainability, in addition to the massive amounts of waste and tailings being produced (Calvo, Mudd, Valero, & Valero, 2016; Ma, Schott, & Lodewijks, 2017). In this research, stream material separated from ore before it enters the production plant and which is

* Corresponding author.
E-mail addresses: thammiris.hajj@unifal-mg.edu.br (T.M. El Hajj), mauro.gandolla@econs.ch (M.P.A. Gandolla), pscsilva@ipen.br (P.S.C. da Silva), henrique.torquato@jrservicce.com.br (H. Torquato), hdelboni@usp.br (H. Delboni).

https://doi.org/10.1016/j.jsm.2019.04.003
Received 3 January 2019; Received in revised form 15 April 2019; Accepted 30 April 2019
Available online 03 May 2019

stoked in open pits from a niobium mine in Brazil was analyzed. This alteration addresses solutions for two of the main sustainability issues in the mining sector, as discussed previously: less energy consumption in comminution steps and improved recovery of Nb, but the amount of *NPW* increased.

The ore body of this mine is composed of four main lithologies: carbonatite, reolite, nelsonite and amphibolite, which are all mixed together in the ore body. The mineralogy of these rocks differs from one another, there the radioactivity also varies a great deal. Mining currently occurs in the fresh rock because almost all the weathered ore reserves have already been depleted and transition to the fresh rock led to major changes in the process. One of the changes is a new magnetic separation in the crushing system that originates the mass flow from which the samples analyzed in this research were collected, called non-processed waste (*NPW*). The nonmagnetic flow is separated from the ore, which decreases the amount of energy used in the mill and increases the process recovery. The issue with this alteration is the amount of *NPW* being generated in the long term because there is no planned place to store this material, which may cause unanticipated environmental impacts.

The use of the *NPW* as aggregate has already been tested and it was showed that the material complies with the standard ABNT NBR 7211:2009 from the Brazilian Association of Technical Standards (Associação Brasileira de Normas Técnicas, 2009). However, due to the occurrence of naturally radioactivity, its commercialization depends on the Brazilian National Commission of Nuclear Energy's (CNEN) approval (Comissão Nacional de Energia Nuclear, 2014; Comissão Nacional de Energia Nuclear, 2016). However, there are no regulations in Brazil concerning the sale of mining byproducts. Thus, this research aims to better investigate the radiological aspects and possible future uses of *NPW*, taking into account radiation protection, through measurements of the activity concentrations of ^{238}U, ^{232}Th, ^{226}Ra, ^{228}Ra, ^{228}Th and ^{40}K of borehole drilled samples and NPW samples. This work also helps assist in the creation of a database that provides comprehensive NORM information for researchers and regulators as is being done in different countries (Iwaoka & Yonehara, 2012). A shortage of space for tailing dams and the increasing costs of monitoring and licensing mining residues make its use as raw material for other manufacturing chains increasingly attractive (Vieira Zuccheratte, Braccini Freire, & Soares Lameiras, 2017).

2. Materials and methods

2.1. Sampling and sample preparation

A long-term sampling campaign was conducted using a borehole drill rig and the samples from all 53 holes were analyzed. The borehole drilled samples were crushed and sized to achieve the sizes needed for the neutron activation analysis (100% < 0.074 mm) and the gamma spectrometry (100% < 2 mm). Moreover, two different *NPW* (d_{95} = 4.13 cm) sets of samples were obtained from the feed of the pile that already stores *NPW*. Pierre Gy's Theory of Sampling (Pitard, 1993) was observed to ensure that the radiological evaluation would be done properly. In total, each set of samples was classified into one of the following: gravel 1 (top size of 26.5 mm), gravel 0 (top size of 13.2 mm), crushed stone (top size of 6.7 mm) and sand (top size of 1.7 mm).

2.2. Neutron activation analysis

For the determination of uranium and thorium concentrations, approximately 150 mg of each sample was weighed and packed in plastic polyethylene bags. Each batch of samples was irradiated together with two reference materials (RM), USGS STM-2 and NIST SRM 1646a, and a paper filter was pipetted with a standard solution of the elements of interest. Each sample was calculated in relation to each reference material and the final report of the results is the mean value related to each RM. All samples and RMs were irradiated for 8 h in the IEA-R1 research reactor, at IPEN under a thermal neutron flux of 10^{12} cm^{-2} s^{-1}. The cooling time for uranium counting was 7 days and for thorium it was approximately 15 days.

The counting time was 1 h for each sample and RM. Gamma spectrometry was performed by using an EG&G Ortec HP-Ge Gamma Spectrometer detector (AMETEK Inc., USA) and associated electronics, with a resolution of 0.88 and 1.90 keV for ^{57}Co (122 keV) and ^{60}Co (1332 keV), respectively (International Atomic Energy Agency, 1990).

Table 1
Lithological domain of each borehole drilled sample, activity concentrations (*AC*) and expanded uncertainty (k = 2) for ^{238}U, ^{226}Ra and ^{232}Th, in Bq/kg.

Sample #	Lithological domain	^{238}U		^{226}Ra		^{232}Th	
		Bq/kg	±	Bq/g	±	Bq/kg	±
1	PHY I	43.1	9.1	33.0	2.5	727.3	65.1
2	CB I	19.5	3.2	59.8	2.8	606.1	54.3
3	PHY II	26.4	8.4	75.1	3.7	562.0	50.9
4	MIS	217.1	23.3	22.0	7.6	1864.2	159.6
5	CB I	nd		54.6	1.5	1792.9	12.6
6	CB II	66.4	18.3	61.6	6.2	1099.2	94.5
7	PHY I	15.1	7.8	80.7	3.7	282.6	2.1
8	AMP II	77.6	12.5	68.1	7.6	1472.8	133.4
9	MIS	Nd		56.0	2.2	227.7	19.6
10	CB I	29.7	8.6	146.6	8.6	804.6	66.3
11	CB II	nd		28.5	5.7	702.7	39.5
12	CB II	nd		134.6	2.7	2332.5	203.0
13	PHY I	90.3	9.9	153.6	5.5	2039.3	181.8
14	CB II	205.0	28.5	52.3	6.7	2933.9	282.0
15	PHY II	98.3	9.3	72.2	5.1	499.0	45.2
16	AMP II	42.5	10.6	56.0	5.7	226.6	1.6
17	AMP II	nd		44.4	3.9	954.4	78.6
18	AMP I	121.7	7.1	111.4	2.9	192.0	1.4
19	CB I	105.6	13.3	52.3	6.7	253.1	23.5
20	PHY I	0.0	0.0	78.4	2.8	1298.6	113.0
21	CB I	16.5	10.5	39.2	5.3	221.3	20.1
22	PHY I	nd		87.0	8.7	1630.4	135.8
23	PHY II	142.7	28.2	43.1	4.6	573.8	49.3
24	PHY I	1898.7	103.9	65.3	4.0	278.6	24.9
25	AMP II	nd		58.6	8.9	1220.4	8.6
26	PHY I	nd		88.3	5.5	1109.7	92.4
27	MIS	117.4	11.0	232.1	2.4	984.5	87.8
28	PHY II	56.6	8.6	128.2	3.8	870.4	78.8
29	AMP I	70.5	8.2	63.1	2.2	314.3	17.7
30	PHY II	29.7	8.6	32.4	3.0	804.6	66.3
31	CB II	65.7	27.2	67.9	8.9	5056.1	283.1
32	PHY I	64.2	7.5	87.0	2.3	555.5	31.2
33	CB II	13.6	4.6	87.6	3.3	718.9	40.3
34	CB I	77.4	16.1	808.9	24.3	641.5	57.4
35	PHY I	41.8	8.9	74.3	2.1	597.0	53.4
36	CB II	nd		130.6	9.4	1764.9	145.4
37	AMP II	70.2	3.7	76.1	6.7	517.9	45.1
38	PHY II	49.7	10.1	70.5	7.5	298.6	26.6
39	AMP I	nd		89.1	8.8	1867.7	155.5
40	AMP I	110.2	9.0	92.1	7.5	520.4	46.6
41	MIS	40.5	12.9	108.2	4.2	1381.6	123.2
42	PHY I	62.5	5.2	75.5	2.4	818.7	46.0
43	AMP II	32.2	4.8	69.6	3.4	933.1	52.4
44	CB I	nd		121.4	8.5	3343.5	290.9
45	CB I	nd		71.7	2.7	1885.4	168.8
46	MIS	67.8	8.4	134.0	4.1	1267.3	71.0
47	MIS	nd		47.6	2.6	1759.7	153.1
48	PHY I	41.1	9.5	52.2	4.1	318.4	29.6
49	AMP I	81.7	12.5	145.3	7.9	806.0	66.4
50	AMP I	10.7	6.8	47.9	2.1	357.9	31.9
51	CB II	152.1	46.9	85.7	8.1	2689.7	224.1
52	PHY I	29.8	8.4	45.4	7.2	530.2	43.7
53	CB I	234.0	110.4	124.5	7.4	2962.6	246.7
Average		89.4		94.2		1141.0	
Standard deviation		259.8		107.3		955.9	

nd = not determined.

Table 2
Lithological domain of each borehole drilled sample, activity concentrations (*AC*) and expanded uncertainty ($k = 2$) for ^{228}Th, ^{228}Ra and ^{40}K, in Bq/kg.

Sample #	Lithological domain	^{228}Th		^{228}Ra		^{40}K	
		Bq/kg	±	Bq/kg	±	Bq/kg	±
1	PHY I	555.0	4.0	562.0	4.0	1680.0	11.0
2	CB I	732.1	13.3	740.5	6.6	2039.2	14.3
3	PHY II	741.7	12.9	752.6	6.4	1878.9	11.8
4	MIS	1880.6	19.2	1930.8	13.6	1324.5	11.9
5	CB I	1811.9	17.3	1832.5	9.6	1432.3	12.6
6	CB II	1158.2	14.4	1062.2	9.8	1642.9	12.8
7	PHY I	292.6	5.5	296.4	1.8	2627.9	15.2
8	AMP II	1857.7	19.4	1688.0	13.5	1582.7	13.5
9	MIS	236.5	8.8	250.9	4.2	657.9	9.1
10	CB I	386.9	8.2	667.8	8.3	425.3	13.0
11	CB II	788.5	11.3	755.8	7.6	1752.1	12.2
12	CB II	2028.7	19.3	2103.2	10.2	706.7	11.0
13	PHY I	2028.6	28.5	2099.1	11.3	1738.4	22.4
14	CB II	3118.9	44.0	3445.3	25.1	1006.0	17.2
15	PHY II	482.2	8.4	484.7	7.3	2266.8	22.2
16	AMP II	212.2	7.9	204.8	4.8	1271.0	11.2
17	AMP II	809.4	11.5	831.9	6.9	1348.3	17.8
18	AMP I	206.4	8.8	224.2	4.0	1443.6	12.7
19	CB I	3118.9	44.0	3445.3	25.1	1006.0	17.2
20	PHY I	1178.4	3.4	1200.4	8.3	1791.8	13.8
21	CB I	282.7	7.6	259.5	5.1	1235.3	10.7
22	PHY I	1422.6	13.6	1462.1	11.4	1918.7	21.1
23	PHY II	587.3	7.5	594.3	5.7	1668.3	12.0
24	PHY I	319.2	3.7	330.2	5.9	1813.8	18.9
25	AMP II	1179.0	14.2	1207.0	10.7	1710.7	20.4
26	PHY I	1091.4	14.8	1101.9	8.0	2383.5	15.3
27	MIS	1103.6	10.5	1123.7	8.1	1609.4	13.7
28	PHY II	907.7	9.2	910.6	6.5	1908.5	11.5
29	AMP I	530.5	6.3	886.2	7.0	2252.0	14.4
30	PHY II	696.1	4.6	717.7	4.7	1866.2	12.3
31	CB II	3812.4	32.3	3496.7	22.1	1356.1	12.5
32	PHY I	884.8	14.0	906.9	7.1	1630.4	11.1
33	CB II	572.8	7.3	562.9	5.7	536.1	6.4
34	CB I	5699.9	47.6	5927.2	58.2	16798.7	129.3
35	PHY I	651.6	6.7	666.5	6.2	2025.5	10.9
36	CB II	2004.4	6.3	2050.4	9.9	1247.7	18.5
37	AMP II	497.7	14.5	507.5	6.4	1772.5	17.4
38	PHY II	1716.2	18.2	1559.6	12.5	1441.0	12.4
39	AMP I	2168.1	22.2	2008.5	15.3	1269.0	13.3
40	AMP I	476.9	14.4	486.5	7.0	1568.5	18.7
41	MIS	1433.1	11.3	1459.6	8.9	1961.5	14.5
42	PHY I	890.2	14.0	895.0	7.1	2191.3	14.5
43	AMP II	971.9	13.4	991.2	7.2	1694.0	12.9
44	CB I	2894.2	29.9	2977.4	16.0	792.8	18.6
45	CB I	1880.8	14.0	1910.6	10.7	2011.2	15.5
46	MIS	914.0	9.2	926.1	7.0	1969.7	12.0
47	MIS	1688.5	6.5	1714.6	9.5	583.9	10.4
48	PHY I	292.8	7.7	198.6	4.2	2016.9	11.5
49	AMP I	1093.2	20.3	1116.6	10.0	1740.7	19.7
50	AMP I	407.1	6.3	413.6	5.0	1698.8	12.4
51	CB II	3075.9	27.5	2806.2	19.1	878.8	11.5
52	PHY I	589.2	10.5	539.0	7.0	2139.0	13.6
53	CB I	2902.0	26.0	2675.1	18.0	1100.6	11.7
Average		1306.9		1320.2		1856.9	
Standard deviation		1084.5		1093.4		2149.9	

The analysis of the data was carried out by using in-house gamma ray software (the VISPECT program) to identify the gamma-ray peaks. The methodology evaluation was performed by cross-checking the reference materials and synthetic standards.

2.3. Gamma spectrometry

For gamma spectrometry the samples were sealed in plastic cans (50 ml), in order to avoid radon loss, for at least 30 days before the measurement to ensure equilibrium between ^{226}Ra and its short half-life progeny. Specific sample activities were determined using a HPGe detector, model GX 2020, from Canberra Industries. The reference materials RGU, RGTh and RGK, from IAEA, were used for efficiency calibration and calibrated sources of ^{60}Co, ^{137}Cs, ^{152}Eu and ^{241}Am, were used for energy calibration. For the determination of ^{226}Ra activity concentration, the mean value of three photopeaks of its progeny, 295 keV and 352 keV of ^{214}Pb and 609 keV of ^{214}Bi, were taken. The Lower Limit of Detection (LLD) for this measurement configuration was 1.8 Bq/kg. For ^{228}Ra activity concentration determination, the mean values of the photopeaks in 338 keV and 911 keV of ^{228}Ac were used (LLD of 3.6 Bq/kg), and the mean values of the photopeaks in 238 keV of ^{212}Pb and 727 keV of ^{212}Bi were used for the determination of ^{228}Th activity concentration (LLD of 4.0 Bq/kg). The photopeak in 1460 keV energy was used to directly determine ^{40}K activity concentration (LLD of 17 Bq/kg).

Table 3
NPW activity concentrations (*AC*) and expanded uncertainty ($k = 2$) for ^{238}U, ^{226}Ra and ^{232}Th, in Bq/kg.

NPW Sample	^{238}U		^{226}Ra		^{232}Th	
	Bq/kg	±	Bq/kg	±	Bq/kg	±
Gravel 1 – Batch 1	47.0	7.0	157.0	9.0	2223.0	134.0
Gravel 0 – Batch 1	45.0	8.0	115.0	7.0	1044.0	63.0
Crushed stone – Batch 1	80.0	10.0	160.0	9.0	1495.0	90.0
Sand – Batch 1	142.0	14.0	233.0	14.0	2091.0	126.0
Gravel 1 – Batch 2	81.4	6.1	56.9	2.7	1249.0	70.0
Gravel 0 – Batch 2	88.7	6.3	42.4	1.9	1529.4	85.7
Crushed stone – Batch 2	71.2	11.3	57.4	3.2	1650.5	102.0
Sand – Batch 2	16.4	9.2	64.8	2.5	1049.9	53.5
Gravel 1 – Average	64.2	6.6	107.0	5.9	1736.0	102.0
Gravel 0 – Average	66.9	7.2	78.7	4.4	1286.7	74.4
Crushed stone – Average	75.6	10.6	108.7	6.1	1572.8	96.0
Sand – Average	52.8	7.7	124.7	6.4	2660.0	159.6

Table 4
NPW activity concentrations (*AC*) and expanded uncertainty ($k = 2$) for ^{228}Th, ^{228}Ra and ^{40}K, in Bq/kg.

NPW Sample	^{228}Th		^{228}Ra		^{40}K	
	Bq/kg	±	Bq/kg	±	Bq/kg	±
Gravel 1 – Batch 1	2290.0	285.0	2189.0	273.0	1369.0	87.0
Gravel 0 – Batch 1	1042.0	130.0	1025.0	128.0	2095.0	135.0
Crushed stone – Batch 1	1254.0	156.0	1205.0	150.0	1745.0	112.0
Sand – Batch 1	1814.0	226.0	1713.0	214.0	1387.0	89.0
Gravel 1 – Batch 2	738.4	9.2	689.1	6.3	834.3	9.9
Gravel 0 – Batch 2	901.7	15.2	843.6	5.7	868.5	8.7
Crushed stone – Batch 2	819.6	11.3	725.2	8.6	947.0	11.4
Sand – Batch 2	854.2	8.5	800.4	6.8	852.5	8.0
Gravel 1 – Average	1514.2	147.1	1439.0	139.6	1101.6	48.5
Gravel 0 – Average	971.9	72.6	934.3	66.8	1481.8	71.8
Crushed stone – Average	1036.8	83.7	965.1	79.3	1346.0	61.7
Sand – Average	1645.9	84.1	1558.5	77.8	807.3	35.6

2.4. Radiological hazard indices

For the activity concentration of natural uranium, thorium and potassium, their specific activity of 12.437 Bq/kg and 4.057 Bq/kg, respectively, was used considering an isotopic abundance of 99.2742% for ^{238}U, 100% for ^{232}Th and 0.0117% for ^{40}K (NPL Report IR 6, 2008).

Radium equivalent activity (Ra_{eq}) was defined as the weighted sum of ^{238}U, ^{232}Th and ^{40}K activities, based on the assumption that 370 Bq/kg of ^{238}U, 259 Bq/kg of ^{232}Th and 4810 Bq/kg of ^{40}K gives an absorbed dose of 1.5 mGy per year, equal to 1 mSv annual effective dose (Tufail,

Table 5
Radiological hazard indices radium equivalent activity (Ra_{eq}), external hazard index (H_{ex}), internal hazard index (H_{in}) and absorbed dose rate (D) – borehole drilled samples.

Sample #	Ra_{eq}	H_{ex}	H_{in}	D
	Bq/kg			nGy/h
1	1202	3.2	3.3	525
2	1084	2.9	3.1	479
3	1023	2.8	3.0	453
4	2790	7.5	7.6	1191
5	2729	7.4	7.5	1168
6	1760	4.8	4.9	761
7	687	1.9	2.1	318
8	2296	6.2	6.4	987
9	465	1.2	1.4	205
10	1330	3.6	4.0	571
11	1168	3.2	3.2	511
12	3524	9.5	9.9	1500
13	3204	8.7	9.1	1375
14	4325	11.7	11.8	1838
15	940	2.6	2.7	421
16	478	1.3	1.4	216
17	1513	4.1	4.2	653
18	497	1.3	1.6	228
19	492	1.3	1.5	219
20	2073	5.6	5.8	895
21	451	1.2	1.3	203
22	2566	6.9	7.2	1105
23	992	2.7	2.8	436
24	603	1.6	1.8	274
25	1936	5.2	5.4	836
26	1859	5.0	5.3	810
27	1764	4.8	5.4	769
28	1520	4.1	4.5	665
29	686	1.9	2.0	313
30	1327	3.6	3.7	579
31	7403	20.0	20.2	3142
32	1007	2.7	3.0	444
33	1157	3.1	3.4	497
34	3020	8.2	10.3	1462
35	1084	2.9	3.1	479
36	2751	7.4	7.8	1178
37	953	2.6	2.8	422
38	608	1.6	1.8	273
39	2858	7.7	8.0	1222
40	957	2.6	2.8	422
41	2235	6.0	6.3	966
42	1415	3.8	4.0	621
43	1534	4.1	4.3	666
44	4964	13.4	13.7	2109
45	2923	7.9	8.1	1256
46	2098	5.7	6.0	909
47	2609	7.0	7.2	1109
48	663	1.8	1.9	301
49	1432	3.9	4.3	627
50	690	1.9	2.0	309
51	4000	10.8	11.0	1701
52	968	2.6	2.7	430
53	4446	12.0	12.3	1893
Average	1869.0	5.0	5.3	810.2
Standard deviation	1367.9	3.7	3.8	579.9

2012). Ra_{eq} was calculated from the following relation (Eq. (1)) proposed by Beretka and Mattew (1985):

$$Ra_{eq} = C_U + 1.43C_{Th} + 0.077C_K \quad (1)$$

where C_U, C_{Th} and C_K are the activity concentrations of ^{238}U, ^{232}Th and ^{40}K, in Bq/kg, respectively.

The external hazard index (H_{ex}), proposed by Hewamanna, Sumithrarachi, Mahawatte, Nanayakkaraand Ratnayake (2001), is applied for a house with walls of finite thickness, windows and doors, and

Table 6
Radiological hazard indices radium equivalent activity (Ra_{eq}), external hazard index (H_{ex}), internal hazard index (H_{in}) and absorbed dose rate (D) – *NPW* samples.

NPW Samples	Ra_{eq}	H_{ex}	H_{in}	D
	Bq/kg			nGy/h
Gravel 1 – Batch 1	3392.7	4.6	9.6	1452
Gravel 0 – Batch 1	1742.1	2.3	5.0	760
Crushed stone – Batch 1	2017.5	2.7	5.9	875
Sand – Batch 1	2789.4	3.8	8.2	1200
Gravel 1 – Batch 2	1106.5	1.5	3.1	477
Gravel 0 – Batch 2	1316	1.8	3.7	565
Crushed stone – Batch 2	1167	1.6	3.3	504
Sand – Batch 2	1275	1.7	3.6	549
Gravel 1 – Average	2249.6	3.0	6.4	964.5
Gravel 0 – Average	1528.8	2.1	4.3	662.5
Crushed stone – Average	1592.5	2.1	4.6	689.3
Sand – Average	2415.6	3.2	6.9	1032.6

can be calculated as Eq. (2):

$$H_{ex} = C_U/370 + C_{Th}/259 + C_K/4810 \quad (2)$$

The radiation hazard due to H_{ex} will be negligible if its value is less than unity. Additionally, the internal hazard index (H_{in}), as defined in Valan, Mathiyarasu, Sridhar, Narayanan, and Arumainathan (2014), takes also into consideration internal exposure due to radon and its short-lived decay products as a threat to the respiratory system. It is calculated as Eq. (3):

$$H_{in} = C_U/185 + C_{Th}/259 + C_K/4810 \quad (3)$$

The external gamma absorbed dose rate (D), related to the risk due to the amount of ionizing radiation, deposited in a body per unit of time, that arises from terrestrial gamma emitters can be derived (nGy h^{-1}) from the measured activity concentrations and the following conversion factors, as given by UNSCEAR (2010) and shown in Eq. (4):

$$D = 0.462C_U + 0.604C_{Th} + 0.0417C_K \quad (4)$$

2.5. Statistical analysis

Univariate and multivariate statistical analyses were applied to the results for data interpretation. The Pearson Correlation Coefficient, in which the correlation coefficient (r) is used to measure association strengths, was used to verify the relationship between the natural radionuclide activity concentrations and the mineral composition of the samples (Devore, 1995; Hupp, Marshall, Campbell, Smith, & Mcguffin, 2008). Hierarchical cluster analyses were applied with the purpose of assembling objects based on their similarities. This goal is achieved by sorting cases into groups or clusters, resulting in a strong association between members of the same cluster and a weak association between members of different clusters (Otto, 1998).

3. Results and discussion

3.1. Radiological characterization

Table 1 and Table 2 show the lithological domain of each borehole drilled sample and activity concentrations (AC) for ^{238}U, ^{226}Ra, ^{232}Th, ^{228}Th, ^{228}Ra and ^{40}K, in Bq/kg and their respective expanded uncertainty ($k = 2$). Table 3 and Table 4 show the AC for the same radionuclides in the NPW samples and their respective expanded uncertainty ($k = 2$). The uncertainty of the results was obtained by means of error propagation with 95% confidence. The lithological domain abbreviations shown in Tables 1 and 2 correspond to the following:

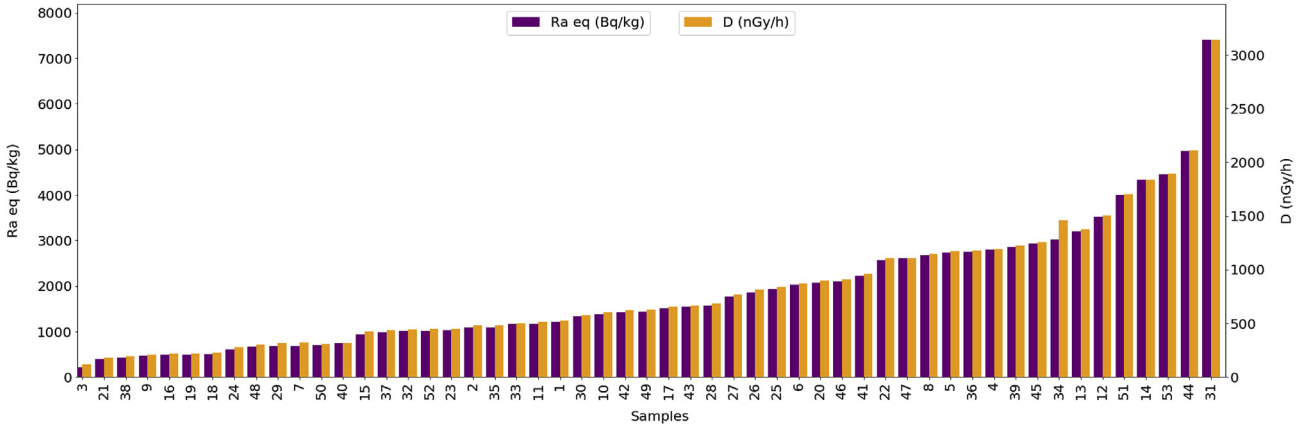

Fig. 1. Radium equivalent (Ra_{eq}) and absorbed dose rate (D) for the borehole drilled samples.

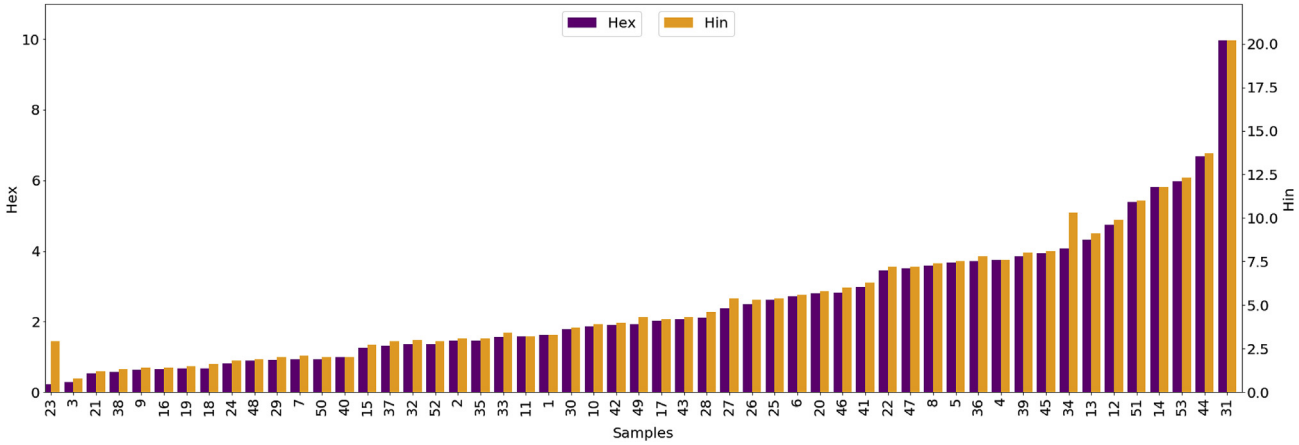

Fig. 2. External (H_{ex}) and internal (H_{in}) hazard indices for the borehole drilled samples.

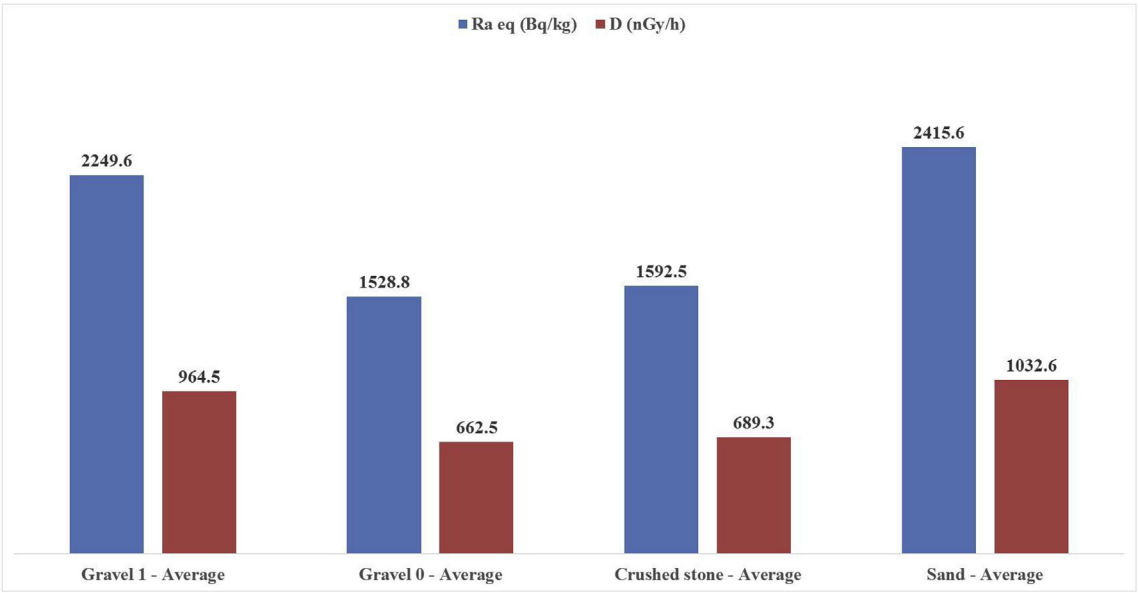

Fig. 3. Radium equivalent (Ra_{eq}) and absorbed dose rate (D) for the *NPW* samples.

PHY is all the phyllite domains within the mine; CB I and CB II are carbonatites; MIS are those which correspond to a mixture of different domains; and AMP I and AMP II are amphibolites. For the borehole drilled samples the *AC* (in Bq/kg) were, on average, 89 ± 260 of ^{238}U (ranging from 10.7 to 1898.7), 94 ± 107 of ^{226}Ra (ranging from 22.0 to 808.9), 1141 ± 956 of ^{232}Th (ranging from 192.0 to 5056.1), 1307 ± 1085 of ^{228}Th (ranging from 206.4 to 5699.9), 1320 ± 1093 of ^{228}Ra (ranging from 198.6 to 5927.2) and 1857 ± 2150 of ^{40}K (ranging from 423.3 to 16798.7), the values followed by the ± sign are the standard deviations. The activity concentrations found are much

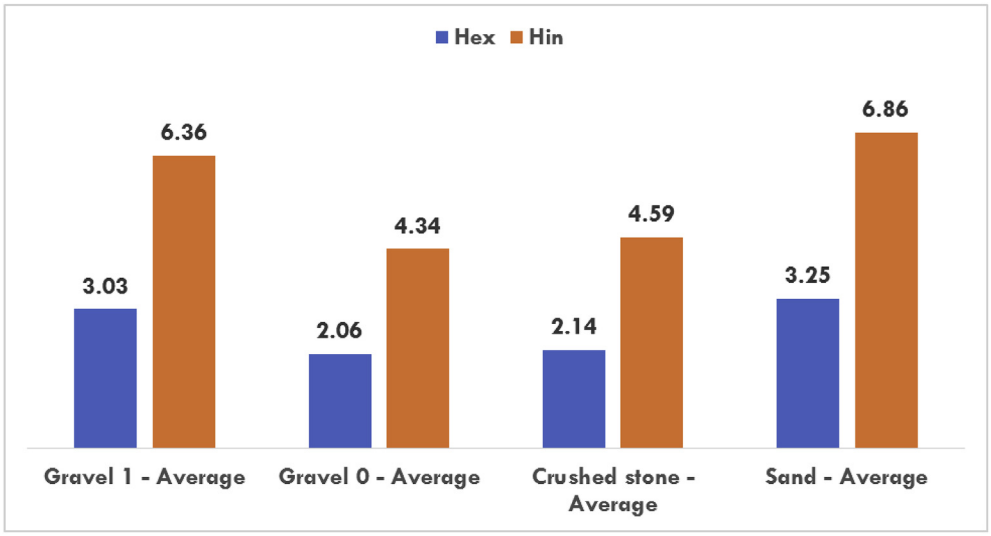

Fig. 4. External (H_{ex}) and internal (H_{in}) hazard indices for *NPW* samples.

Table 7
Spearman Rank Order Correlations – marked correlations are significant at $p < 0.05$.

Variable	Ra_{eq} (Bq/kg)	H_{ex}	H_{in}	D (nGy/h)
Pyrochlore	0.04	0.04	0.07	0.05
Kalipyrochlore	−0.31	−0.31	−0.3	−0.32
Ferrous cordierite	−0.2	−0.2	−0.19	−0.19
Magnetite	−0.07	−0.07	−0.08	−0.06
Ankerite	0.33	0.33	0.33	0.33
Magnesian Calcite	−0.04	−0.04	−0.06	−0.05
Phlogopite	−0.07	−0.07	−0.07	−0.08
Biotite	0.3	0.3	0.28	0.31
Orthoclase	0.4	0.4	0.4	0.39
Alkali feldspar	**0.77**	**0.77**	**0.77**	**0.77**
Siderite	0.31	0.31	0.32	0.31
Richterite	−0.24	−0.24	−0.25	−0.23
Quartz	−0.18	−0.18	−0.18	−0.17
Calcite	−0.16	−0.16	−0.16	−0.16
Hydroxyapatite	0.04	0.04	0.04	0.04
Anquerite	**0.42**	**0.42**	**0.44**	**0.43**
Sanidine	−0.09	−0.09	−0.08	−0.09
Ferrous phlogopite	−0.32	−0.32	−0.32	−0.32
Dolomite	**0.74**	**0.74**	**0.76**	**0.74**
Barytocalcite	**−0.44**	**−0.44**	**−0.44**	**−0.44**

higher than the global average, as presented in UNSCEAR (2010). However, *AC* of the same order of magnitude was also found in other naturally radioactive Th rich mineralization studied in Brazil (Larijani et al., 2017; Alves, Pereira, Neto, & Menegotto, 2018; Hazin, Gazineu, & de Farias, 2008; El Hajj et al., 2017). In this case, it is important to investigate whether the type of rock influences the radionuclides' *AC*s. Therefore, the average for the carbonatite samples and the average for the samples of all others lithological domains was calculated. The *AC* was, on average, 1753.5 Bq/kg for ^{232}Th in the carbonatite samples and 851.8 Bq/kg in all other samples. This fact is important when predicting the radiological profile of the raw material entering the ore treatment plant.

For the *NPW* samples the *AC* (in Bq/kg) were, on average, 64.9 ± 9.4 of ^{238}U (ranging from 16.4 to 142.0), 105 ± 23 of ^{226}Ra (ranging from 42.7 to 233.0), 1814 ± 594 of ^{232}Th (ranging from 1044.0 to 2223.0), 1292 ± 338 of ^{228}Th (ranging from 738.4 to 2290.0), 1224 ± 321 of ^{228}Ra (ranging from 689.1 to 2189.0) and 1184 ± 296 of ^{40}K (ranging from 834.3 to 2095.0). The control of *NPW* composition is a challenge because only in the last few years the control of the ore grade has been done. Due to the great variability in the lithologies and their *AC*, the inclusion of radiological evaluation in the mine planning context for the material that enters the ore treatment plant and consequently the metallurgical process may help to segregate the tailings and to create different possible applications.

3.2. Radiological risk assessment

The radiological hazard index (*RHI*) radium equivalent activity (Ra_{eq}), external hazard index (H_{ex}), internal hazard index (H_{in}) and absorbed dose rate (D) of the samples analyzed in this study are shown in Table 5 and Table 6.

For better visualization, the data was plotted in the graphs in Figs. 1–4. The average results for the borehole drilled sample were 1860.7 ± 1377.6 (Bq/kg) for the Ra_{eq}, 806.6 ± 584.1 (nGy/h) for D, 5.0 ± 3.7 for H_{ex} and 5.3 ± 3.8 for H_{in}. The main conclusions were that all *RHI* showed high standard deviation (the same order of magnitude of the averages) for the borehole drilled samples and this can be explained by the mineralogical composition of the rocks that form the deposit. Both, the borehole drilled samples and the *NPW* samples show values of radiological hazard indices which are higher than the reference values or the global average (370 Bq/kg for Ra_{eq}, H_{ex} and $H_{in} > 1$ and 58 nGy/h (UNSCEAR, 2010)). Therefore, the use of *NPW* without dilution as a general building material, with the same composition as the material researched in the present study, could represent a risk to human health if no boundary use conditions are adopted.

3.3. Multivariate statistical analysis

The Pearson correlation rank was calculated for the *RHI* of each sample and the mineralogical content; the results are shown in Table 7. The results corroborate the initial premise that the carbonatite lithology, bold in the table, was most radiologically hazardous since both the alkali feldspar and the dolomite presented significant correlations with all *RHI*.

Cluster analysis was applied to the radiological indices showed in Table 5. When cutting the obtained dendrogram at a level of 20% of the $100 \cdot D_{link}/D_{max}$, four main groups were observed (Fig. 5). The bold group is the one that corresponds to the highest radiological hazard indices and all the samples are from the carbonatite domains. This result is helpful when sequencing the mine, so the workers would not be exposed to unnecessary risks.

In Fig. 6 the borehole drilled samples were classified in the mine, considering the radiological hazard indices and coordinates of the collars. The red dots in the map represent the highest risk, the yellow

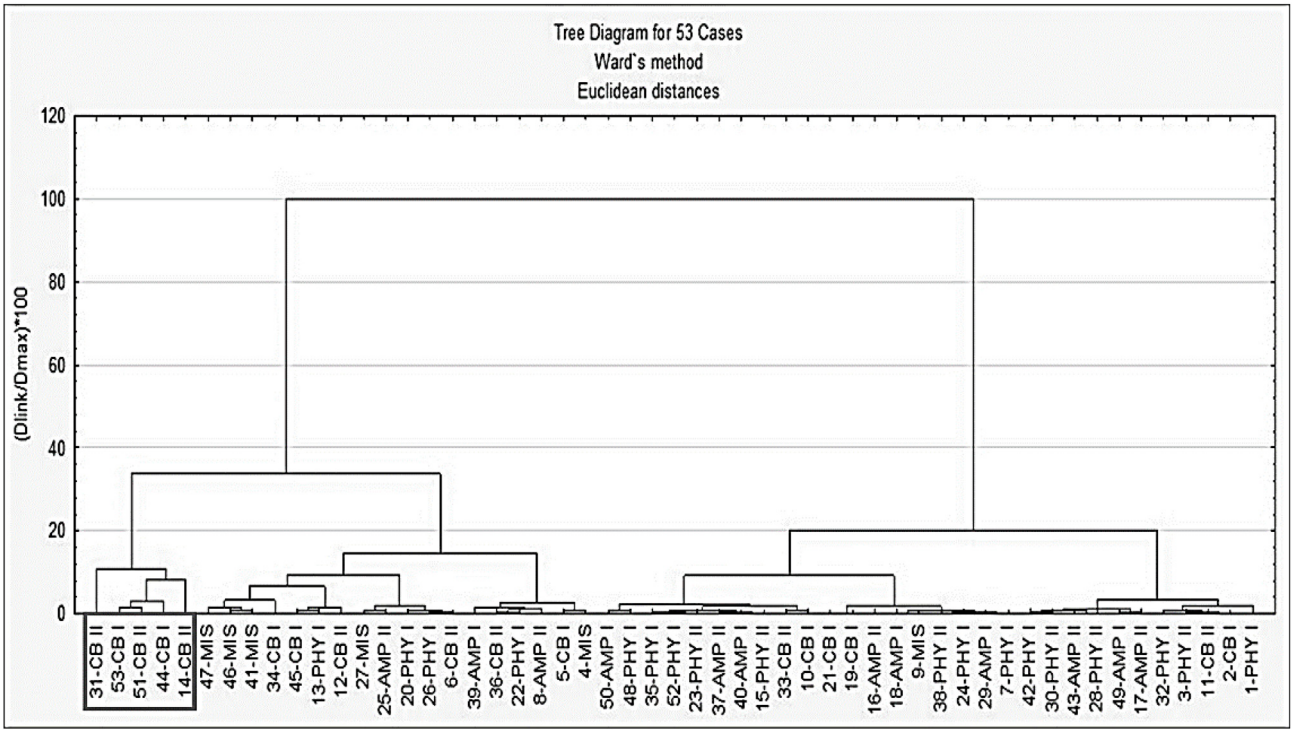

Fig. 5. Dendrogram obtained in cluster analysis considering the radiological risk indices.

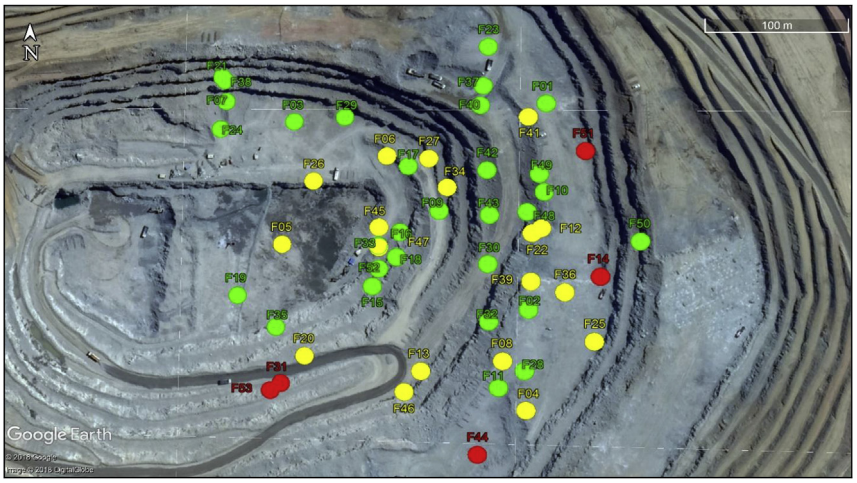

Fig. 6. Boreholes locations, in the open pit mine located at Catalão-GO in Brazil, classified regarding the radiological hazard indices.

ones represent intermediate and the green ones are the ones with low risk.

4. Conclusion

From the analysis of 53 borehole drilled samples, high variability in relation to radioactivity content related to mineralogical characteristics was observed. The lithology denominated by carbonatite is the most critical with regards to the radiological activity in the deposit. Regarding the *NPW*, the radiological hazard indices were higher than the reference values or the global average, so some investigations could be carried out in further studies which would consider the use of diluted *NPW* in cement to produce concrete or its application for roadbed foundation. The re-use of this material would be optimal for minimizing the negative environmental consequences of having the material stacked in a roofless environment, but it should only be done if it is proven to be safe, with regards to radiation protection.

Ethical statement

Authors state that the research was conducted according to ethical standards.Acknowledgments

The authors would like to thank Dr. Boguslaw Michalik from GIG for encouraging the authors to attend the ENA Workshop in 2018. We would like to specially thank the IAEA for the financial support which enabled one of the authors to attend the conference and the technical meeting held by the Agency.

Conflicts of interest

None declared.

Funding

This work is supported by Universidade Federal de Alfenas and

Instituto de Pesquisas Energéticas a Nucleares.

Appendix A. Supplementary data

Supplementary data to this article can be found online at https://doi.org/10.1016/j.jsm.2019.04.003.

References

Alves, M. A. S., Pereira, V. P., Neto, A. C. B., & Menegotto, E. (2018). Weathering of the Madeira world-class Sn-Nb-Ta (Cryolite, REE, U, Th) deposit, Pitinga mine (Amazon, Brazil). *Journal of Geochemical Exploration, 186*, 61–76. https://doi.org/10.1016/j.gexplo.2017.12.003.

Associação Brasileira de Normas Técnicas (2009). *Agregados para concreto – Especificação.* Retrieved November 21, 2018 from https://www.abntcatalogo.com.br/norma.aspx?ID=40092.

Beretka, J., & Mattew, P. J. (1985). Natural radioactivity of Australian building materials, industrial waste sand by-products. *Health Physics, 48*(1), 87–95. https://doi.org/10.1097/00004032-198501000-00007.

Calvo, G., Mudd, G., Valero, A., & Valero, A. (2016). Decreasing ore grades in global metallic mining: A theoretical issue or a global reality? *Resources, 5*, 36. https://doi.org/10.3390/resources5040036.

Comissão Nacional de Energia Nuclear (2014). *Diretrizes básicas de proteção radiológica.* Retrieved November 21, 2017 from http://appasp.cnen.gov.br/seguranca/normas/pdf/Nrm301.pdf.

Comissão Nacional de Energia Nuclear (2016). *Requisitos de Segurança e Proteção Radiológica para Instalações Mínero-Industriais.* Retrieved November 21, 2017 from http://appasp.cnen.gov.br/seguranca/normas/pdf/Nrm401.pdf.

Departamento Nacional de Produção Mineral (2018). *Sumário mineral 2016/ Coordenadores Thiers Muniz Lima, Carlos Augusto Ramos Neves Brasília: DNPM, 2018.* DNPM/MME.

Devore, J. (1995). *Probability and statistics for engineering and sciensces* (4th ed.). Belmont (CA): Duxbury Press.

EC, FAO, ILO, OECD/NEA, PAHO, UNEP, et al. (2014). *Radiation Protection and Safety of radiation sources: International basic safety standards. General safety requirements part, Vol. 3.* Vienna: IAEA.

El Hajj, T., Silva, P., Gandolla, M., Dantas, G., Santos, A., & Delboni, H., Jr. (2017). Radiological hazard indices and elemental composition of Brazilian and Swiss ornamental rocks. *Brazilian Journal of Radiation Sciences, 5*(2)https://doi.org/10.15392%2Fbjrs.v5i2.269.

Ferrira, A. L. R., da Silva, J. N., Lima, C. A. M., & da Silva, F. C. A. (2018). Radiological risk classification of NORM industries in Brazil. *Naturally occurring radioactive material (NORM VIII), proceedings of an international symposium held in Rio de Janeiro, Brazil, 18-21 October 2016. Vienna: International atomic energy agency*.

Garcia C Marques, M., Mohamad El Hajj, T., Maques Braga Junior, J., Chieregati, A., & Delboni Junior, H. (2017). Theory of Sampling and geostatistics for twin drill hole analysis in a niobium mine in Araxá, Brazil. *Eighth world conference on sampling and blending: 9–11 may 2017 Perth, Australia* (pp. 97–105). Carlton, Vic: AusIMM.

Gonçalves de Lima, J. (2010). *Perfil da mineração do nióbio.* Retrieved March 12, 2018 from J Mendo Consultoria: http://www.mme.gov.br/documents/1138775/1256650/P11_RT20_Perfil_da_Mineraxo_do_Nixbio.pdf/48860760-63f2-489e-b4b9-e16236fd1413.

Hazin, C. A., Gazineu, M. H. P., & de Farias, E. E. G. (2008). Uranium and thorium in Zircon sands processed in northeastern Brazil. *IRPA 12: 12 international congress of the international radiation protection association (IRPA): Strengthening radiation protection worldwide, Argentina: SAR.* Retrieved November 10, 2018 from https://inis.iaea.org/search/search.aspx?orig_q=RN:42070516.

Hewamanna, R., Sumithrarachi, C., Mahawatte, P., Nanayakkara, H., & Ratnayake, H. (2001). Natural radioactivity and gamma dose from Sri Lankan clay bricks used in building construction. *Applied Radiation and Isotopes, 54*(2), 365–369. https://doi.org/10.1016/S0969-8043(00)00107-X.

Hupp, A., Marshall, L., Campbell, D., Smith, R., & Mcguffin, V. (2008). Chemometric analysis of diesel fuel for forensic and environmental applications. *Analytica Chimica Acta, 606*(2), 159–171. https://doi.org/10.1016/j.aca.2007.11.007.

International Atomic Energy Agency (1990). *Practical aspects of operating a neutron analysis laboratory.* Vienna: International Atomic Energy Agency.

International Atomic Energy Agency (2013). *Management of NORM residues.* Vienna: International Atomic Energy Agency.

Iwaoka, K., & Yonehara, H. (2012). Database of the radioactivity of NORM used as industrial raw materials. *Radiation Protection Dosimetry, 152*(4), 444–449. https://doi.org/10.1093/rpd/ncs067.

Josef Maringer, F., Baumgartner, A., Cardellini, F., Cassette, P., Crespo, T., Dean, J., ... Vodenik, B. (2017). Advancements in NORM metrology – results and impact of the European joint research MetroNORM. *Applied Radiation and Isotopes, 126*, 273–278. https://doi.org/10.1016/j.apradiso.2017.02.040.

Larijani, C., Schwendner, P., Cockell, C., Ivanov, P., Russell, B., Aitken-Smith, P., et al. (2017). Destructive and non-destructive measurements of NORM in monazite-rich sands of Brazil. *Radiation Physics and Chemistry, 140*, 180–185. https://doi.org/10.1016/j.radphyschem.2017.01.010.

Liu, H., & Pan, Z. (2011). NORM situation on non-uranium mining in China. *Annals of the ICRP, 41*(3–4), 343–351. Elsevier https://doi.org/10.1016/j.icrp.2012.06.015.

Ma, W., Schott, D., & Lodewijks, G. (2017). A new procedure for Deep Sea mining tailings disposal. *Minerals, 7*, 47. https://doi.org/10.3390/min7040047.

NPL Report IR 6 (2008). *Recommended nuclear decay data.* Retrieved December 13, 2018 from http://publications.npl.co.uk/npl_web/pdf/ir6.pdf.

Otto, M. (1998). Multivariate methods. In R. Kellner, J. Mermet, M. Otto, & H. Widmer (Eds.). *Analytical chemistry*. Weinheim: Wiley VCH.

Pitard, F. F. (1993). *Pierre Gy's sampling theory and sampling practice: Heterogeneity, sampling correctness, and statistical process control* (2nd ed.). Florida: CRC Press.

Rangel Alves, A. (2015). *Proposição de um modelo para avaliação do ciclo de vida do nióbio* (PhD Thesis) Sao Paulo, Brazil: Faculdade de Engenharia, Arquitetura e Urbanismo, Universidade Metodista de Piracicaba. Retrieved November 30, 2018 from https://www.unimep.br/phpg/bibdig/aluno/visualiza.php?cod=1368.

Tufail, M. (2012). Radium equivalent activity in the light of UNSCEAR report. *Environmental Monitoring and Assessment, 184*(9), 5663–5667. https://doi.org/10.1007/s10661-011-2370-6.

UNSCEAR (2010). *Sources and effects of ionizing radiation. United nations scientific committee on the effects of atomic radiation UNSCEAR 2000 report ot the general assembly, with scientific annexes (volume I: Sources).* United Nations Publication.

Valan, I., Mathiyarasu, R., Sridhar, S., Narayanan, V., & Arumainathan, S. (2014). Investigation of background radiation level in Krusadai island Mangrove, Gulf of Mannar, India. *Journal of Radioanalytical and Nuclear Chemistry, 304*(2), 735–744. https://doi.org/10.1007/s10967-014-3864-9.

Vieira Zuccheratte, A., Braccini Freire, C., & Soares Lameiras, F. (2017). Synthetic gravel for concrete obtained from sandy iron ore tailing and recycled polyethyltherephtalate. *Construction and Building Materials, 151*, 859–865. https://doi.org/10.1016/j.conbuildmat.2017.06.133.

Vives i Batlle, J., Ulanovsky, A., & Copplestone, D. (2017). A method for assessing exposure of terrestrial wildlife to environmental radon (^{222}Rn) and thoron (^{220}Rn). *The Science of the Total Environment, 605–606*, 569–577. https://doi.org/10.1016/j.scitotenv.2017.06.154.